Shear crack induced debonding failure of FRP-plated RC beams

Ninoslav PESIC
PhD student
University of Sheffield
Sheffield, UK

Kypros PILAKOUTAS
Reader
University of Sheffield
Sheffield, UK

Summary

This work deals with the behaviour of reinforced concrete (RC) beams strengthened in flexure with externally bonded FRP plates. It focuses on an analytical investigation of the shear crack induced plate-end debonding failure. A simple and efficient design criterion is formulated for this failure mode by implementing empirical anchorage strength model for FRP plates bonded to concrete.

The accuracy of the procedure is validated with the available experimental results. The results from the non-linear finite element (FE) analysis are also presented towards the end of the paper.

FE analysis was introduced to provide insight into the complex stress and deformations state in concrete prior to failure which can not be accounted for through the linear elastic analysis.

Keywords: Model code RC design, FRP strengthening, FRP bond strength.

1. Introduction

Externally bonded FRP plates are economical, practical and efficient way of increasing the flexural strength of existing RC beams. However, the flexural capacity of strengthened elements can not often be utilised mainly due to the premature brittle plate-end debonding failures. The most widely investigated type of such failures is caused by the stress concentration in concrete which leads to the crack opening at the plate termination point and separation of the bonded plate from the beam.

A less studied type of brittle plate-end failure considered here is denoted either as “reverse” or “shear crack induced” plate debonding because the critical failure crack through the concrete cover layer is initiated inside the span of FRP-plated RC beams. The reverse debonding is caused or initiated by the critical shear crack from which another horizontal crack propagates towards the end of the bonded FRP-plate.

In terms of design guidelines, the ***fib*** bulletin N.14 [Ref.1] covers the application of externally bonded FRP reinforcement. Still, this document only identifies the shear crack induced debonding failure as the peeling-off caused at shear cracks, but it does not yet provide the analytical method nor practical design criterion.

The shear crack induced debonding failure of FRP-plated RC beams was identified experimentally by Triantafillou and Plevris [2], Garden *et al*.[3], Ahmed and Van Gemert [4], Ramana *et al*.[5], Nguyen *et al*.[6] and Rahimi and Hutchinson [7]. The physical nature of the failure mechanism observed on FRP-strengthened RC beams is closely related to the anchorage strength and the effective transfer length of bonded FRP plates. This means that the design procedure for the shear failure mode in question can be conveniently formulated using one of the available empirical models for the anchorage strength and the effective length of bonded FRP plates which is the line followed in this paper.

Given the non-linear mechanical properties of concrete, any simplified design criterion for the shear crack induced failure alone would not suffice to accurately represent the fracture process taking place through the concrete cover layer and, from this reason, the design procedure should be supported by results from non-linear FE analysis. The evaluation of the overall stress/strain field in the plate anchorage region, the origin of failure through detection of the principal tensile stresses in concrete cover layer are carried out for the sample FE model of one of the documented FRP-strengthened RC beams.

2. Design Criterion

According to the most recent strength model of Chen and Teng [8], the effective anchorage length of FRP plates bonded to concrete, L_e, and the corresponding debonding force, P_{fu}, are estimated from:

$$L_e = f_{ck}^{0.25}\sqrt{E_f t_f} \quad (mm) \tag{1}$$

$$P_{fu} = 0.427\beta_f \beta_L E_f b_f \sqrt{f_{ck}} \quad (N) \tag{2}$$

where E_f and f_{ck} are the elastic modulus of FRP plate and the characteristic compressive strength of concrete (both in *MPa*), and $\beta_f = \sqrt{(2-b_f/b_c)}/\sqrt{(1+b_f/b_c)}$, $\beta_L = sin[\pi L/(2L_e)]$ if $L<L_e$ or $\beta_L=1$ if $L=L_e$, while b_f and t_f are the plate width and thickness and b_c is the width of the concrete beam (all in *mm*).

To implement Equations 1 and 2 into a design criterion specific to the shear crack induced plate debonding, the origin of failure from which the length L_e is measured needs to be specified. From the bending moment diagram, this section is assumed to be where the bending moment due to the applied loading, M, equals the yielding bending moment of the previously unstrengthened beam, M_y.

Thus, the failure through concrete is expected to originate at this critical section when the tensile stress in FRP plate, $\sigma_{f,b}$,exceeds the critical debonding stress characteristic for FRP-plated RC beams, σ_{fd}, and the design criterion can be written in the following form:

$$\sigma_{f,b} \le \sigma_{fd} = \eta_b P_{fu}/(b_f t_f) \quad (N/mm^2) \tag{3}$$

The bond reduction coefficient $\eta_b < 1.0$ is introduced to account for the difference between the bond achieved in pull-out test specimens used to establish Eq.1 and 2 and the debonding mechanism for FRP plates attached to concrete elements deformed in flexure. The value of debonding force P_{fu} from Eq.2 is based on simple shear tests with FRP plates bonded to idealised un-cracked and undeformed concrete blocks (Fig.1-a). In the case of FRP-strengthened beams, the overall bond strength of the FRP-adhesive-concrete medium is inevitably reduced as a result of the beam deformation due to flexure and the presence of shear cracks in the plate anchorage zone (Fig.1-b).

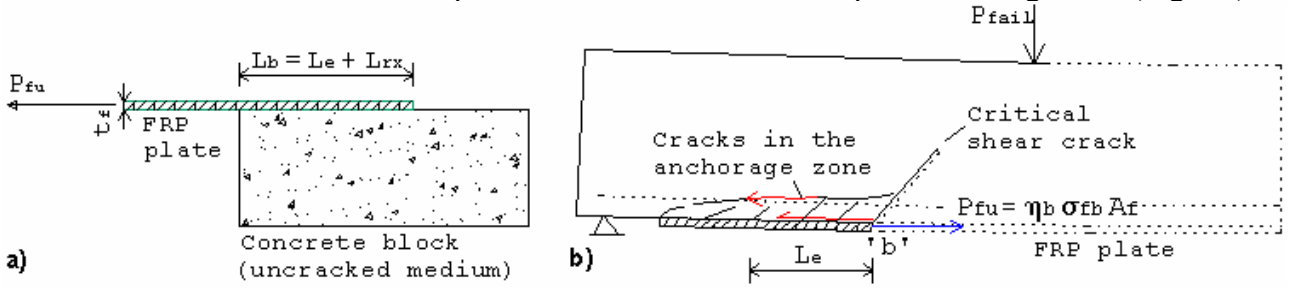

Figure 1: a) Evaluation of debonding force P_{fu} ; b) Reduced bond strength on FRP-plated beams.

3. Validation with Experimental Results

The values of the bond reduction coefficient appearing in Eq.3 are empirically evaluated as $\eta_b = \sigma_{f,b}/\sigma_{fu}$ for experimentally tested RC beams which failed due to shear crack induced. The tensile stresses in the bonded FRP plates at the pre-defined sections 'b', $\sigma_{f,b}$, are obtained from the sectional analysis and the results are listed in Table 1.

Table 1: Evaluation of the design criterion for shear crack induced plate-end debonding failure.

Beam Ref.	P_{fail} [kN]	b/h [mm]	f_{ck} [MPa]	M_y [kNm]	E_f [GPa]	b_f [mm]	t_f [mm]	L_b [mm]	L_e [mm]	$\sigma_{f,d}$ [MPa]	$\sigma_{f,b}$ [MPa]	η_b n/a	$^*\Delta\eta_b$ n/a
Triantafillou and Plevris [2] - (1992)													
B4	14.78	76/127	44.7	1.79	186	63.2	0.65	50	134	260.1	228.0	0.88	-5.68
B5	15.25	76/127	44.7	1.79	186	63.2	0.65	43	134	226.3	228.0	1.02	-22.9
B6	13.95	76/127	44.7	1.79	186	63.3	0.90	53	158	201.7	186.6	0.92	-9.78
Garden *et al.* [3] - (1998)													
Bu4.5	30.00	145/230	47.0	24.36	115	90.0	1.28	772	147	309.2	268.4	0.87	-4.60
Ahmed and Van Gemert [4] - (1999)													
DF.3	60.00	125/225	40.5	14.92	240	75.0	0.50	199	137	697.4	629.4	0.90	-7.78
DF.4	62.75	125/225	40.5	14.92	240	75.0	0.67	188	159	604.0	566.8	0.94	-11.7
Ramana *et al.* [5] - (2000)													
0.52B	10.60	100/100	30.0	0.92	123	10.0	1.40	62	177	203.2	171.5	0.85	-2.35
0.89B	11.60	100/100	30.0	0.92	123	20.0	1.40	54	177	167.0	140.5	0.84	+1.19
1.42B	14.44	100/100	30.0	0.92	123	40.0	1.40	39	177	107.2	102.7	0.96	-13.5
Nguyen *et al.* [6] - (2001)													
C5	23.50	120/150	25.1	10.78	181	80.0	1.20	343	208	332.0	279.5	0.84	+1.19
C10	23.50	120/150	25.1	10.34	181	80.0	1.20	325	208	332.0	287.3	0.86	-3.49
C20	24.50	120/150	25.1	9.47	181	80.0	1.20	271	208	332.0	305.1	0.92	-9.78
Rahimi and Hutchinson [7] - (2001)													
6xA5	31.60	200/150	40.0	9.84	127	150.0	0.80	226	127	361.6	264.0	0.73	+12.0
2xA6	29.70	200/150	40.0	9.84	127	150.0	1.20	246	155	295.2	213.5	0.72	+13.2

$^*\Delta\eta_b = 100 \cdot (\eta_{b,av.} - \eta_b)/\eta_{b,av.}$

After the mandatory introduction of the partial safety factors for the applied loading and material properties, and until more experimental and statistical data is available, it is recommended that the design criterion defined by Eq.3 should incorporate the lower limit value of $\eta_b=0.70$ instead of the average value $\eta_{b,av.}=0.83$ obtained for the set of 20 examined beams (Fig.2-a).

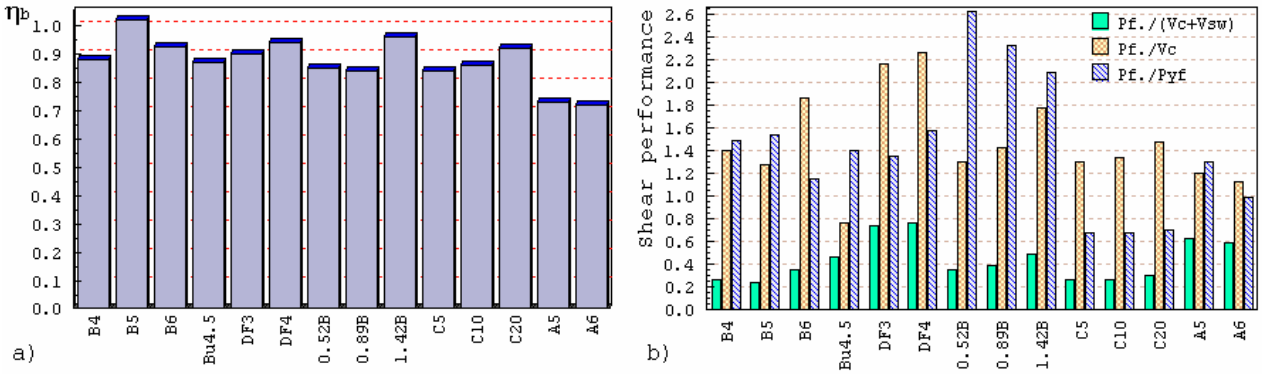

Figure 2: The evaluation of the coefficient ; b) Shear performance of FRP-plated beams.

4. Shear Performance of Strengthened Beams

The experimental results are also used to assess the shear performance of the examined beams in a more traditional model code approach. The values of the three ratios P_{fail}/V_c, $P_{fail}/(V_c+V_{sw})$ and P_{fail}/P_y are graphically presented in Fig.2-b. Here, P_{fail} is the applied shear force at failure and P_y is the shear force corresponding to the yielding bending moment of FRP-plated beam while the

characteristic shear strengths provided by concrete, V_c, and internal steel links, V_{sw}, are calculated in accordance to the ACI design code [9].

The most significant observation that could be made on the basis of resulting graph is that no single beam has achieved its nominal shear capacity as the $P_{fail.}/(V_c+V_{sw})$ ratio is always smaller than *1.0* when the shear crack debonding failure takes place. As the design code equations appear to be insufficient, the focus is reverted next to the finite element method as a more accurate way of predicting the stress-deformation states leading to this type of brittle failures.

5. Non-Linear Finite Element Analysis

Based on the smeared crack concrete fracture model, the two-dimensional non-linear FE analysis is conducted to determine the stress concentration in the concrete layer within the plate anchorage zone prior to failure. Beam DF.4 tested by Ahmed and Van Gemert [4] is chosen as a sample model and the commercial finite element software ADINA [10] is employed in the analysis.

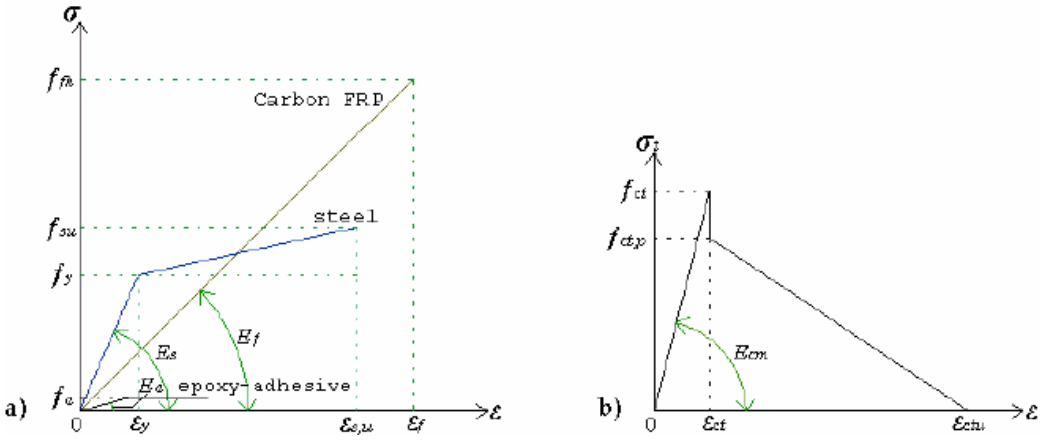

Figure 3: Constitutive mat. models: a) steel/CFRP reinforcement, adhesive; b) concrete in tension.

The analytical material properties for the adhesive layer, steel and FRP reinforcement are shown in Fig.3-a. The constitutive uniaxial material law for concrete in tension, adopted in the analysis, is illustrated in Fig.3-b. It is a modification to the Hillerborg 's original cohesive model [11] defined by the concrete ultimate tensile strength, f_{ct}*=3.4 MPa*, the elastic modulus, E_{cm}, the post-cracking tensile stress, $f_{ct,p}$, and the value of the *mode I* fracture energy adopted as $G_{f,I}$*=0.75 N/mm*^{2}. To account for the weakening behaviour of concrete under increased compressive stresses, the stress-strain relations for biaxial stress states given by Kupfer and Gerstle [12] are adopted.

The origin of failure and the direction of the critical crack propagation towards the plate termination points can be traced through the load history plots of principal tensile stresses in concrete, σ_{p1}.

Fig.4 shows the σ_{p1} contour plots for the two characteristic load stages during which the damage in the shear span of the beam reaches the concrete cover layer below internal steel reinforcing bars. These history plots provide evidence of the transition of the maximum tensile stresses in concrete towards the plate termination points where the failure finally takes place when the concrete strength in tension is exceeded.

6. Conclusions

The anchorage strength model for FRP plates was modified with the introduction of the bond reduction coefficient and was calibrated with tested FRP-strengthened beams to formulate the design criterion for shear crack induced failures. To be compared with the critical debonding stress, the key parameter in the proposed analytical procedure is the tensile stress in bonded FRP plates calculated at the critical section 'b' at which the failure is considered to originate. Relying on the verification with a limited number of published experimental results, the approximate method is suitable for quick design calculations and analytical assessment of RC beams strengthened in flexure with FRP plates.

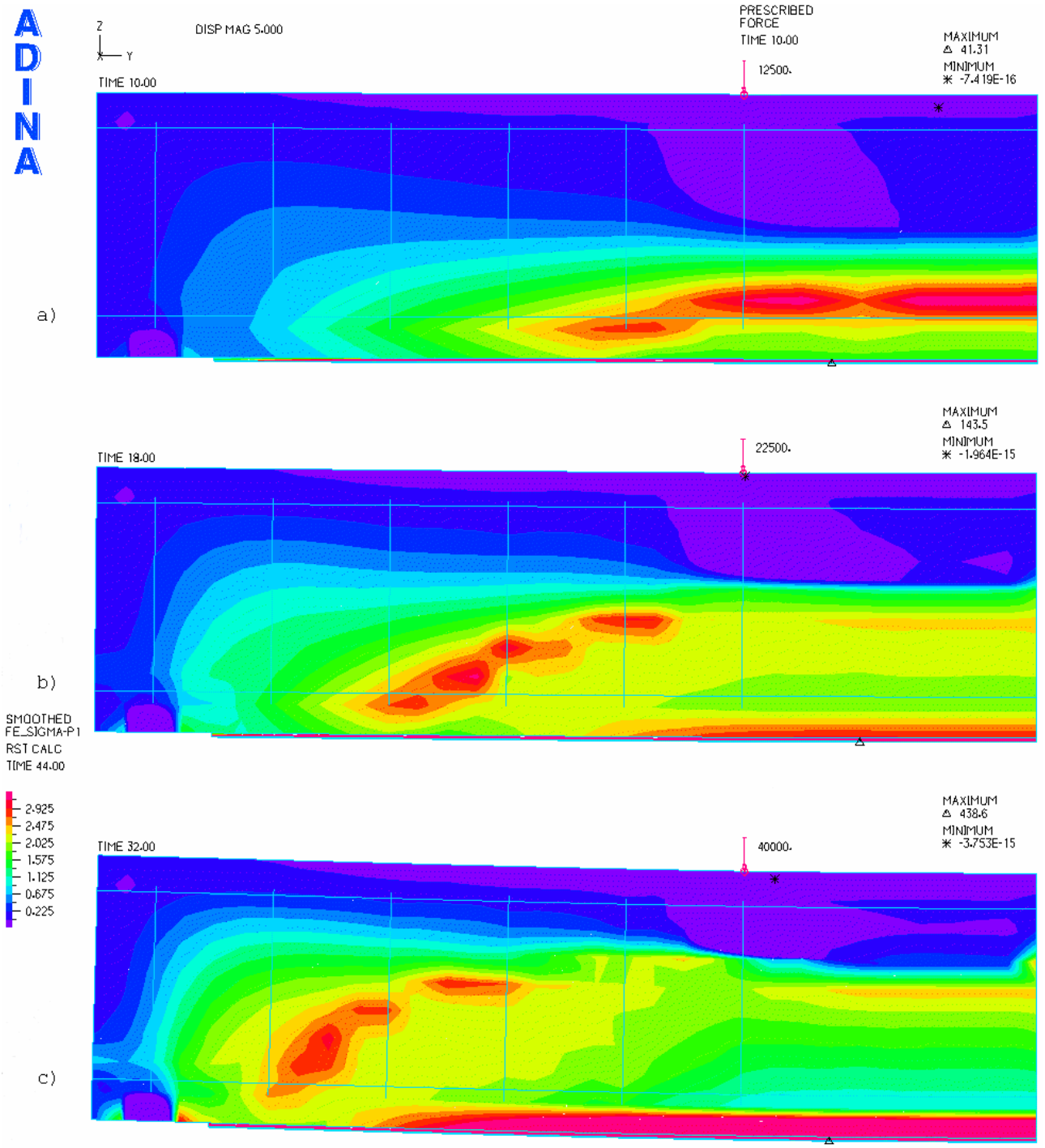

Figure 4: The loading history of principal tensile stresses in concrete for beam DF.4 [4] subjected to: a) 20%; b) 36%; c) 64% of the final failure load of 2 x 62.5 kN (stress values in MPa).

The results from non-linear finite element analysis using smeared fracture model for concrete were additionally used to help in identifying the mode of failure. The FE analysis revealed that, for the reverse or shear crack induced debonding, the higher stress concentration first builds up at the level of internal steel reinforcement and not on the concrete-adhesive interface nor at the plate-end point as would be the case with the majority of plate-end failures involving concrete cover separation.

Acknowledgments

The authors would like to express their gratitude to the British Universities O.R.S. awarding body for providing the financial support to the first author and also to the E.U.Commission for funding the TMR research network "ConFibreCrete".

References

[1] "Externally bonded FRP reinforcement for RC structures", Bulletin No.14, *fib* (CEB-FIP), Lausanne, Switzerland, 2001.

[2] Triantafillou T.C. and Plevris N., "Strengthening of RC beams with epoxy-bonded fibre-composite materials", *RILEM Materials and Structures*, 1992, Vol.25, No.148, p.201-211.

[3] Garden H.N., Quantrill R.J., Hollaway L.C., Thorne A.M. and Parke G.A.R., "Experimental study of the anchorage length of carbon fibre composite plates used to strengthen RC beams", *ELSEVIER Construction and Building materials*, 1998, Vol.12, No.4, p.203-219.

[4] Ahmed O. and Van Gemert D., "Effect of longitudinal carbon fiber reinforced plastic laminates on shear capacity of reinforced concrete beams", *Procs. FRPRCS 4 - Fiber Reinforced Polymer Reinforcement for Reinforced Concrete Structures*, Baltimor, USA, 1999, p.933-944.

[5] Ramana V.P.V., Kant T., Morton S.E., Dutta P.K., Mukherjee A. and Desai Y.M., "Behavior of CFRP strengthened reinforced concrete beams with varying degrees of strengthening", *ELSEVIER Composites Part B: Engineering*, 2000, Vol.31, No.6-7, p.461-470.

[6] Nguyen D.M., Chan T.K. and Cheong H.K., "Brittle failure and bond development length of CFRP-concrete beams", *ASCE Journal of Composites for Construction*, 2001, Vol.5, No.1, p.12-17.

[7] Rahimi H. and Hutchinson A., "Concrete beams strengthened with externally bonded FRP plates", *ASCE Journal of Composites for Construction*, 2001, Vol.5, No.1, p.44-56.

[8] Chen J.F. and Teng J.G., "Anchorage strength models for FRP and steel plates bonded to concrete", *ASCE Journal of Structural Engineering*, 2001, Vol.127, No.7, p.784-791.

[9] "Building code requirements for structural concrete (ACI 318-02) and Commentary (ACI 318R02), *American Concrete Institute*, Detroit, USA, 2002.

[10] ADINA, *FEA Software and User's Manual v8.0*, ADINA R&D Inc., http://www.adina.com, Marylend, USA, 2002.

[11] Hillerborg A., Moder M. and Petterson P.E., "Analysis of crack formation and crack growth in concrete by means of fracture mechanics", *PERGAMON Cement and Concrete Research*, 1976, Vol.6, No.6, p.773-782.

[12] Kupfer H.B. and Gerstle K.H., "Behavior of concrete under biaxial stresses", *ASCE Journal of the Engineering Mechanics Division*, 1973, Vol.99, No.4, p.853-866.